EUROPEAN ORGANIZATION FOR NUCLEAR RESEARCH

CERN-EP/87-199
October 28th, 1987

ANGULAR DISTRIBUTIONS OF MUON PAIRS PRODUCED BY NEGATIVE PIONS ON DEUTERIUM AND TUNGSTEN

NA10 Collaboration

M. Guanziroli, D.A. Jensen[a],
P. Le Coultre, H. Suter, V.L. Telegdi,
ETH, Zurich, Switzerland.

K. Freudenreich[b],
CERN, Geneva, Switzerland.

A. Ereditato, P. Strolin,
Università di Napoli and INFN Sezione di Napoli, Naples, Italy.

P. Bordalo[c], Ph. Busson, L. Kluberg, A. Romana,
R. Salmeron, C. Vallée,
Ecole Polytechnique, Palaiseau, France.

J.J. Blaising[d], A. Degré[d], P. Juillot,
R. Morand[d], M. Winter,
CRN and Université Louis Pasteur, Strasbourg, France.

ABSTRACT

We present the angular distributions of high-mass muon pairs produced in a high-statistics experiment by 140 and 194 GeV/c π^- beams impinging on a tungsten target, and by 286 GeV/c π^- beam on deuterium and tungsten targets. We find no evidence for a center-of-mass energy dependence or a nuclear dependence of the angular distribution parameters. The two parameters λ and μ are found to be essentially independent of any kinematical variable. In contrast, the parameter ν increases with the dimuon transverse momentum P_T, at variance with recent perturbative QCD predictions. Our statistics at large x_1 are insufficient to substantiate the higher-twist prediction.

(Submitted for publication to Zeitschrift für Physik C)

---

a) Permanent address: Dept of Physics and Astronomy, University of Massachusetts, Amherst, MA, USA.

b) Now at ETH, Zurich, Switzerland.

c) Now at LIP, Lisbon, Portugal.

d) Now at LAPP, Annecy-le-Vieux, France.

1. Introduction

In a recently published article [1], we have presented the angular distributions of high-mass ($M > 4$ GeV/c^2) muon pairs produced by 194 GeV/c pions on a tungsten target. These angular distributions are parametrized as:

$$d\sigma/d\Omega \sim 1 + \lambda\cos^2\theta + \mu\sin 2\theta\cos\phi + {}^1/_2\nu\sin^2\theta\cos 2\phi, \quad (1)$$

where θ and ϕ are the polar and azimuthal angles of the muons in the dimuon rest frame. The main result of our analysis was, in addition to an estimate of the parton intrinsic transverse momentum, a determination of the ratio of annihilation with hard-gluon emission to the sum of annihilation with hard-gluon emission and Compton scattering; we furthermore showed that the data were consistent with, but not sufficient to prove, the higher-twist hypothesis of Berger et al. [2].

To determine the above-mentioned ratio, we had used in [1] semi-empirical formulae based on theoretical calculations (cf. [1] for a complete list of references) taking into account only the "hard component", i.e. the first-order, hard-gluon contribution, of the cross-section. These formulae gave a good description of the data, yielding for the above ratio a value ranging from 58 to 75%, in agreement with that (70 to 85%) given by a computation in the next-to-leading logarithm approximation. However, this agreement was fortuitous, since according to that calculation, the "hard component" accounted only for some 10% of the total cross-section.

Taking advantage of recent progress in the soft-gluon resummation technique, Chiappetta and Le Bellac [3] subsequently reanalyzed the dependence of the angular distribution parameters on the dimuon transverse momentum P_T. They found that the departure from the "naïve" Drell-Yan values $\lambda = 1$, $\mu = 0$, and $\nu = 0$ is expected to be less than 0.05 for P_T up to 3 GeV/c, much smaller than that observed [1, 4, 5]. They also noted that the agreement between the experimental data and the hard-component distribution must be accidental, since the latter contributes only for 10% to the total cross-section. The simple formulae used in [1], which took only the hard component into account, are therefore not theoretically justified. Conversely, perturbative QCD in its present status fails to reproduce the P_T dependence of the parameter ν.

The analysis of the 194 GeV/c data presented in [1] has now been refined and extended to the other two beam momenta where we took data, namely, 140 and 286 GeV/c. The 286 GeV/c data from a deuterium target have also been analyzed. The differences in the set-up and in the analysis with respect to [1] will be presented in the next section, the results discussed in Sect. 3 and the conclusions presented in Sect. 4.

2. Set-up and Analysis

The NA10 set-up used to collect the 194 GeV/c data at the CERN SPS has already been described in detail elsewhere [1, 6]. We shall therefore mention here only the modifications introduced for the 140 and 286 GeV/c data taking.

The NA10 spectrometer had primarily been designed for scaling studies: in order to keep the acceptance essentially independent of the beam momentum, it could be expanded (or contracted) along the beam direction. The acceptances in the angular variables $\cos\theta$ and ϕ were thus similar at the three beam momenta. Most of the data were taken with a 12 cm tungsten target, a shorter target being used for 30% of the 194 GeV/c data and 40% of the 286 GeV/c data in 1985. For the 140 and 286 GeV/c runs, a 120 cm long liquid-deuterium target was added 2 m upstream of the tungsten target. The vertex resolution was such that only 0.5% of the events actually originating from the deuterium target could be improperly assigned to the tungsten target. No corresponding correction was therefore applied to the data.

The 286 GeV/c data were collected over two separate periods, viz. in 1983 and in 1985. These two sets of data were analyzed separately to check for possible differences (the apparatus was contracted for the 140 GeV/c data taking in 1984, and then expanded again). As they were found to be consistent, they were added, after correcting for the acceptances. The 140 GeV/c data were also taken under two different running conditions, namely, with normal magnetic field and at a field reduced by 30%. These two sets were also checked for consistency and added after correcting for the acceptances.

In the previous analysis [1], we computed the angular distributions in three different reference frames, viz. the Gottfried-Jackson (GJ), the Collins-Soper [7] (CS), and the u-channel (UC) frames (see [1] for a definition of these frames and of the kinematical variables and angles). Using kinematical relations, we transformed the values from two of these frames to the third one, and averaged them in

that frame. However, a subsequent extensive Monte-Carlo study of the smearing and biases introduced by the finite resolution of the apparatus, the spread in beam momentum, and the Fermi motion, indicated that the angular resolution is better in the CS frame ($\Delta\cos\theta = 0.03$) than in the other two ($\Delta\cos\theta = 0.04$ in the UC frame and $\Delta\cos\theta = 0.06$ in the GJ frame). In addition, a comparison of the generated values of $\cos\theta$ with the reconstructed ones revealed that the latter might be slightly biased in the GJ and UC frames.

Another concern regarding the analysis is the effect of nuclear reinteractions, i.e. the contamination of the data samples by secondary pions originating either from the deuterium or from the tungsten target and producing in the latter a muon pair within the acceptance of the spectrometer. Such reinteraction events are assigned a wrong beam momentum (that of the primary pions) and affect both the absolute normalization (which may be ignored here as we are not discussing absolute cross-sections) and the shape of the differential distributions. A comparison of target-full vs. target-empty data, for the deuterium target, and of long-target vs. short-target data, for the tungsten target, as well as a special Monte-Carlo analysis (using the known production cross-sections for the deuterium and a cascade simulation for the tungsten), showed that the fraction of high-mass muon pairs due to secondary pions interacting in the tungsten target is $(14\pm4)\%$ for the 286 GeV/c data, $(4\pm2)\%$ for the 194 GeV/c data, and $(4\pm3)\%$ for the 140 GeV/c data. The $\cos\theta$ distribution of secondary induced events was found from the Monte-Carlo studies to be similar to that of primary induced events in the CS frame, but concentrated at low values of $|\cos\theta|$ in the two other frames. A study of this distribution in the CS frame yields for the systematic error in λ at most 0.07 for the 286 GeV/c data. For the 194 GeV/c data, where the deuterium target was absent, this error is twice smaller, and less than 0.01 for the 140 GeV/c data. As these systematic errors are smaller than the statistical uncertainties on λ (typically ≥ 0.10), no allowance for them was made. On the other hand, the fraction of secondaries is independent of ϕ. The systematic errors possibly induced on μ or ν are at 286 GeV/c (the worst case) at most of order 0.015, to be compared with typical statistical uncertainties larger than 0.02. Here again, no allowances were made.

For the deuterium target, where only secondaries originating from that target need to be considered, the fraction of secondary muon pairs is $(8\pm2)\%$ for the 286 GeV/c data, so that the systematic errors induced by reinteractions are about twice smaller than for the tungsten events at that beam momentum.

We pointed out above that the resolution smearing and the nuclear reinteraction biases are least important in the CS frame; we shall therefore use *only this frame* in the present analysis. For the dependence of the angular distribution parameters on x_1 (the fractional momentum of the quark in the pion), where the theoretical predictions [2] are made for the GJ frame, we transform the parameters to that frame using relations (6) of [1].

The effect of the nuclear reinteractions on the angular distributions being found independent of the relative longitudinal momentum x_F, we did not apply any cut on that variable. On the other hand, we discarded events with $x_1 \geq 0.7$, in order to suppress a possible higher-twist effect. Unfortunately, this cut rejected most events with masses above the Υ. No correction was applied for a possible contamination by heavy-flavour decays, as the fraction of like-sign dimuon events was smaller than 1% in the kinematical region for all three beam momenta.

Table 1 summarizes the data-taking conditions for the different periods; the number of dimuons given is the number of events with $4.0 \leq M \leq 8.5$ GeV/c^2 ($4.05 \leq M \leq 8.5$ GeV/c^2 for the 194 GeV/c data) and $M \geq 11$ GeV/c^2 (M is the dimuon mass).

The angular distribution is parameterized as [1]:

$$(1/N)\,\Delta N/\Delta\Omega = 1 + \lambda\cos^2\theta + \mu\sin 2\theta\cos\phi + {}^1/_2\nu\sin^2\theta\cos 2\phi + \alpha\cos\theta + \beta\sin\theta\cos\phi + \gamma\sin\theta\sin\phi, \qquad (2)$$

where N is the total number of events, and ΔN the number of events (corrected for the acceptance) in a cell $\Delta\Omega = \Delta\cos\theta\Delta\phi$. The six parameters were estimated by fitting the corrected distribution to (2) by means of a least-square method, for several intervals of certain kinematical variables. For each such interval the data were distributed in 6 bins in $\cos\theta$ ($-0.5 \leq \cos\theta \leq 0.5$) times 5 bins in ϕ ($-\pi \leq \phi \leq \pi$), i.e. in 30 cells. Cells containing less than 20 events were not used. As the lever arm in $\cos\theta$ is limited, we need rather large statistics in each interval for a reliable determination of the angular distribution parameters, especially of λ: we therefore discarded the intervals with less than about one thousand events. For the remaining intervals the χ^2/d.o.f. were all between 0.5 and 1.5. In the previous analysis of the 194 GeV/c data [1], the events were distributed in 10×20 cells; in the intervals with relatively small statistics, a large number of cells were not sufficiently populated, and λ was biased toward low values. Such a bias is avoided in the present analysis. The systematic errors were estimated to be at most of the order of the statistical uncertainties. The asymmetry parameters α, β, and γ, which corre-

spond to terms odd under coordinate inversion, were small and presumably due to experimental effects not included in the Monte-Carlo (e.g. nuclear reinteraction effects, beam angle). Alternatively, assuming that $dN/d\Omega$ must be even under inversion, one may keep in (2) only the terms in λ, μ, and ν and fold the $\cos\theta$, ϕ distribution over the region $\cos\theta \geq 0$. We checked that this latter method yields similar results.

A description of the Monte-Carlo and further details on the analysis can be found in [1].

3. Results and Discussion

The dependence of the parameters λ, μ, and ν on the center-of-mass energy $\sqrt{s}$, on the transverse momentum P_T, and on the dimensionless variables $\rho \equiv P_T/M$, $\sqrt{\tau} \equiv M/\sqrt{s}$, y (the rapidity), and x_1, are given in Tables 2 to 7 and displayed on Figs. 1 to 6 for the tungsten target.

The 286 GeV/c deuterium data are compared in Fig. 8 with tungsten data taken at the same momentum. The parameters from both targets agree very well for all kinematical variables, so that we find *no evidence* for a nuclear dependence. In the following, we shall therefore consider only the tungsten data, where the statistics are about ten times larger.

We first show the dependence of the parameters averaged over all kinematical variables for each center-of-mass energy (Table 2 and Fig. 1). Within the statistical uncertainties the three parameters are consistent with the average values $\langle\lambda\rangle = 0.90 \pm 0.03$, $\langle\mu\rangle = -0.008 \pm 0.007$, and $\langle\nu\rangle = 0.089 \pm 0.007$ (shown as dashed lines on Fig. 1). The deviation of λ from 1 can be used to estimate the intrinsic transverse momentum K_T of the parton inside a hadron; with the relation [1]:

$$\langle K_T^2 \rangle = \langle M^2 \rangle (1-\lambda)/2(\lambda+3), \tag{3}$$

we find $\langle K_T^2 \rangle = 0.3 \pm 0.1(\text{stat.}) \pm 0.1(\text{syst.})$ $(\text{GeV/c})^2$. Since the values of λ at the three energies have a larger than statistical spread about their mean, we prefer to quote a limit, viz. $\langle K_T^2 \rangle \leq 0.6$ $(\text{GeV/c})^2$ at the 90% confidence level. The value of μ, compatible with zero, indicates that both hadrons contribute equally to the transverse momentum P_T of the dimuon.

The ρ dependence of the parameters is given in Table 3 and on Fig. 2. The behaviour of the parameters is similar for the three beam momenta. In particular, ν increases markedly with ρ, whereas λ and μ are independent of ρ. Fitting the values of ν to the empirical formula:

$$\nu(\rho) = \varepsilon\rho^2/(1+\varepsilon\rho^2) \tag{4}$$

we obtain for the coefficient ε: 1.46 ± 0.27 (χ^2/d.o.f.$=5.0/4$), 1.84 ± 0.17 (χ^2/d.o.f.$=3.6/4$), and 1.17 ± 0.17 (χ^2/d.o.f.$=6.0/4$) for the 140, 194, and 286 GeV/c data respectively (average value $\langle\varepsilon\rangle = 1.50\pm0.11$). The results of these fits are shown as dot-dashed curves on Fig. 2. For the deuterium data we find $\varepsilon = 1.9\pm0.7$ (χ^2/d.o.f.$=3.4/4$), in agreement with the tungsten values. Using the above results and the relation [8]:

$$\lambda = 1-2\nu, \tag{5}$$

which is analogous to the Callan-Gross relation [9] in deep inelastic scattering, we compute the corresponding curves for $\lambda(\rho)$ (also shown on Fig. 2). These curves *fail to reproduce the data*, with χ^2's of 9.2, 17.5, and 19.2 respectively for 5 d.o.f. As relation (5) is expected to hold for perturbative QCD, this discrepancy between the behaviour of λ and that of ν suggests that the observed variation of ν with ρ, or equivalently with P_T (see below), could be a *non-perturbative effect*. No corresponding violation of the Callan-Gross relation, which in contrast to (5) is modified by perturbative QCD, has been observed in deep inelastic scattering [10]. The violation of (5) can neither be due to the intrinsic momentum of the partons, which would affect λ rather than ν [1], and would not depend on ρ, nor to a higher-twist effect of the type predicted in [2], as the high-x_1 region is excluded here, and furthermore this would again affect λ rather than ν. The comparison with the deuterium data (Fig. 8 b), which exhibit the same trend, shows that this is not a nuclear effect.

To allow a comparison with theoretical predictions [3], we give in Table 4 and on Fig. 3 the P_T dependence of the parameters, which is quite similar to the ρ dependence discussed above. We have superposed on Fig. 3 the results of these calculations which took into account not only the "naïve" Drell-Yan and the first-order, hard-gluon contributions but also the soft-gluon contributions summed to all orders. These calculations make use of set I of structure functions from [11], assuming $\Lambda = 200$ MeV, but are however not very sensitive to any particular choice of parameters. They correspond to fixed values of $\sqrt{s}$, M, and y, but the variation of the angular distribution parameters with M (or $\sqrt{\tau}$) and y is smooth enough (see below) to justify the comparison with data integrated over these variables. We made the computation for the three center-of-mass energies, using the relevant average mass ($\langle M\rangle = 5.0$ GeV/c^2), and rapidities ($\langle y\rangle = 0.15$, 0.36, and 0.42 respectively). The result of these computations are shown as dashed curves on Fig. 3. As the zeroth-order contribution, together with the soft-gluon contribution, accounts for 90% of the total cross-section, and as the soft gluons hardly

affect the angular distribution parameters at all, these predictions deviate very little from the values $\lambda = 1$, $\mu = 0$, $\nu = 0$ given by the "naïve" Drell-Yan model. The observed values of λ and μ are in good agreement with the expected values. On the other hand, the large values of ν observed at $P_T > 1$ GeV/c are *in disagreement with the perturbative QCD predictions.* Assuming systematic errors to be equal to the statistical uncertainties and adding them in quadrature, a χ^2 test yields probabilities of $6 \cdot 10^{-3}$, $< 10^{-5}$, and $3 \cdot 10^{-4}$ at 140, 194, and 286 GeV/c respectively for the observed values of ν to agree with the predicted ones. In view of this large discrepancy, we did not attempt to fine-tune the calculations by varying the structure functions or any other parameters (renormalization constant Λ, scale of the running coupling constant, etc.).

In an earlier paper [12] we have shown, by a comparison of deuterium and tungsten data that nuclear effects can contribute some 60 MeV/c to the values of P_T measured in tungsten. As these effects are small, we did not correct the values of P_T used in the present analysis. Such a correction would anyhow *increase* the discrepancy between the predicted and observed values of ν.

Table 5 and Fig. 4 give the dependence of the parameters λ, μ, and ν on the scaling variable $\sqrt{\tau}$. The values of λ and μ are independent of this variable over the range $0.16 \leq \sqrt{\tau} \leq 0.50$. The constancy of λ indicates that there is no higher-twist effect at $x_1 < 0.7$ (remember that the data with $x_1 > 0.7$ are excluded here), since such an effect would induce a M^{-2n} dependence. On the other hand, ν decreases with $\sqrt{\tau}$ for $\sqrt{\tau} < 0.3$.

The dependence of the parameters on the rapidity y is given in Table 6 and Fig. 5. No significant variation is observed.

Finally, we give in Table 7 and Fig. 6 the dependence of the parameters on x_1, the fractional momentum of the parton in the pion. No clear variation of the parameters with x_1 is observed, except for a 1.5σ decrease of λ in the last interval of the 286 GeV/c data. To check the compatibility of the data with the higher-twist hypothesis of Berger et al. [2], we transformed the values of λ to the GJ frame, using relations (6) of [1]. To improve the statistical significance of the data, we averaged the values of λ for the three energies (Fig. 7). These average values were fitted to the relation:

$$\lambda(x_1) = [\lambda'(1-x_1) - \eta^2]/[(1-x_1) + \eta^2], \qquad (6)$$

giving $\lambda' = 1.04 \pm 0.14$, and $\eta^2 = 0.064 \pm 0.047$ (χ^2/d.o.f. = 0.2/3) (dashed curve, Fig. 7). This value differs from $\eta^2 = 0$ (i.e., λ independent of x_1) by less than 1.4σ, and does not allow to draw a conclusion as to

the existence of a higher-twist effect at large x_1. The fact that one cannot make a statistically significant statement about this effect is further illustrated by the fitting of a straight line to the data, as indicated by a dot-dashed line on Fig. 7, yielding a slope of -0.36 ± 0.25.

4. Conclusions

We have presented the angular distributions of dimuons produced in π-tungsten interactions at 140, 194, and 286 GeV/c, and in π-deuterium interactions at 286 GeV/c. The 194 GeV/c data have already been published [1], but the large number of $(\cos\theta, \phi)$ cells used in that analysis induced a bias in the determination of λ. The present analysis should be free of such a bias and the following conclusions supersede those of [1].

The behaviour of the parameters λ and μ agrees well with that predicted by perturbative QCD, with the inclusion of soft-gluon emission [3]: λ is close to 1, and substantially independent of any kinematical variable. In the GJ frame, there is a suggestion of a decrease of λ with x_1, as predicted by the higher-twist hypothesis [2]; however, we have few events at high x_1, where that hypothesis applies. An intrinsic transverse momentum squared of the parton inside the hadron is determined to be smaller than 0.6 $(\mathrm{GeV/c})^2$ (90% C.L.). Also, μ is close to zero in the CS frame, as expected if both annihilating partons contribute equally to the transverse momentum of the dimuon. The most striking result of this analysis is the strong dependence of ν on P_T [or equivalently on ρ: $\nu(\rho) \approx 3\rho^2/(2+3\rho^2)$], in *clear disagreement* with the perturbative QCD expectations [3]. As a corresponding decrease of λ with P_T, expected if the Callan-Gross-type relation $1-\lambda=2\nu$ holds, is not observed, we conclude that this unexplained effect is perhaps of non-perturbative origin. A comparison of tungsten and deuterium data shows that the angular distribution parameters are independent of the type of target nucleus.

We are indebted to Prof. M. Le Bellac and Dr P. Chiappetta for a discussion on their theoretical work, and for making their computer program available to us. We thank Prof. G. Preparata for a enlightening discussion.

References

[1] S. Falciano et al., Z. Phys. C, Particles and Fields **31**, 513 (1986).

[2] E.L. Berger and S.J. Brodsky, Phys. Rev. Lett. **42**, 940 (1979); E.L. Berger, Phys. Lett. **89B**, 241 (1980); Z. Phys. C, Particles and Fields **4**, 289 (1980); S.J. Brodsky, E.L. Berger, and G.P. Lepage, *Proceedings of the Drell Yan Workshop,* Fermilab (1982), p.187, and references therein.

[3] P. Chiappetta and M. Le Bellac, Z. Phys. C, Particles and Fields **32**, 521 (1986).

[4] J. Badier et al., Z. Phys. C, Particles and Fields **11**, 195 (1981); O. Callot, *Thèse de doctorat d'Etat*, Orsay Report LAL 81/05 (1981), unpublished.

[5] J.S. Conway, *Ph.D. Thesis*, University of Chicago, (June, 1987), unpublished.

[6] L. Anderson et al., Nucl. Instr. Methods **223**, 26 (1984).

[7] J.C. Collins and D.E. Soper, Phys. Rev. **D16**, 2219 (1977).

[8] J.C. Collins, Phys. Rev. Lett. **42**, 291 (1979); C.S. Lam and W.K. Tung, Phys. Rev. **D18**, 2447 (1978); K. Kajantie, J. Lindfors, and R. Raitio, Phys. Lett. **74B**, 384 (1978), and Nucl. Phys. **B144**, 422 (1978); C.S. Lam and W.K. Tung, Phys. Lett. **80B**, 228 (1979).

[9] C.G. Callan and D.J. Gross, Phys. Rev. Lett. **22**, 156 (1969).

[10] R. Voss, *Rapporteur talk at the International Symposium on Lepton and Photon Interactions at High Energies*, Hamburg, July 27 – 31, 1987, to appear in the Proceedings.

[11] D.W. Duke and J.F. Owens, Phys. Rev. **D30**, 49 (1984), and **D30**, 943 (1984).

[12] P. Bordalo et al., Phys. Lett. **193B**, 373 (1987).

Table 1: Summary of data taking conditions

Beam momentum [GeV/c]	$\langle\sqrt{s}\rangle$ [GeV]	Target lengths [cm]	Number of dimuons ($\times 10^3$)
140 (10kA)	16.2	12.0	23.9
140 (7kA)	16.2	12.0	21.8
194	19.1	5.6, 12.0	147.7
286 (1983)	23.2	12.0	46.5
286 (1985)	23.2	5.6, 12.0	37.6
286 (Deuterium)	23.2	120.0	8.3

Table 2: Parameters λ, μ, and ν in the CS frame as a function of $\sqrt{s}$

Interval [GeV]	$\langle\sqrt{s}\rangle$ [GeV]	Events ($\times 10^3$)	λ	μ	ν
15.7 – 17.4	16.2	45.7	1.01±0.08	0.002±0.020	0.082±0.016
18.5 – 20.5	19.1	147.7	0.83±0.04	0.008±0.010	0.091±0.009
22.6 – 25.0	23.2	84.1	0.99±0.06	−0.027±0.010	0.090±0.012

Table 3: Parameters λ, μ, and ν in the CS frame as a function of ρ

$\sqrt{s}$ [GeV]	Interval	$\langle\rho\rangle$	Events ($\times 10^3$)	λ	μ	ν
16.2	0.00 – 0.10	0.06	9.7	0.92±0.17	−0.011±0.039	−0.012±0.034
	0.10 – 0.20	0.15	16.1	1.16±0.12	0.027±0.032	0.085±0.026
	0.20 – 0.30	0.25	10.4	1.09±0.17	0.002±0.038	0.059±0.032
	0.30 – 0.40	0.34	5.4	0.64±0.23	0.022±0.053	0.154±0.045
	0.40 – 1.20	0.50	4.2	0.88±0.23	−0.119±0.068	0.256±0.052
19.1	0.00 – 0.10	0.06	30.0	0.90±0.09	0.036±0.022	−0.013±0.020
	0.10 – 0.20	0.15	50.4	0.83±0.07	−0.013±0.017	0.024±0.015
	0.20 – 0.30	0.25	34.6	0.77±0.09	0.022±0.020	0.121±0.018
	0.30 – 0.40	0.34	17.8	0.87±0.12	−0.051±0.030	0.167±0.026
	0.40 – 1.20	0.51	14.9	0.79±0.13	0.047±0.035	0.327±0.028
23.2	0.00 – 0.10	0.06	15.9	0.90±0.13	−0.024±0.030	0.016±0.027
	0.10 – 0.20	0.15	27.1	0.96±0.10	−0.029±0.023	0.049±0.021
	0.20 – 0.30	0.25	19.3	1.08±0.12	−0.026±0.027	0.092±0.024
	0.30 – 0.40	0.34	10.7	0.98±0.15	−0.037±0.040	0.161±0.033
	0.40 – 1.20	0.53	11.0	1.09±0.16	−0.013±0.041	0.203±0.033

Table 4: Parameters λ, μ, and ν in the CS frame as a function of P_T

$\sqrt{s}$ [GeV]	Interval [GeV/c]		$\langle P_T \rangle$ [GeV/c]	Events ($\times 10^3$)	λ	μ	ν
16.2	0.00 –	0.50	0.32	9.2	0.87±0.18	0.060±0.041	0.002±0.035
	0.50 –	1.00	0.74	16.2	1.20±0.13	0.003±0.032	0.079±0.026
	1.00 –	1.50	1.23	11.2	0.99±0.16	−0.051±0.037	0.074±0.032
	1.50 –	2.00	1.72	5.6	0.96±0.22	0.042±0.054	0.184±0.044
	2.00 –	6.00	2.44	3.6	0.65±0.26	−0.046±0.070	0.150±0.055
19.1	0.00 –	0.50	0.32	27.3	0.87±0.10	0.049±0.023	0.001±0.021
	0.50 –	1.00	0.75	49.2	0.80±0.07	−0.012±0.017	0.012±0.016
	1.00 –	1.50	1.23	36.5	0.85±0.08	−0.003±0.020	0.113±0.018
	1.50 –	2.00	1.72	19.8	0.76±0.11	0.011±0.028	0.209±0.024
	2.00 –	6.00	2.52	14.8	0.87±0.12	0.037±0.035	0.307±0.025
23.2	0.00 –	0.50	0.32	14.5	0.89±0.13	−0.011±0.031	0.042±0.028
	0.50 –	1.00	0.75	26.3	0.89±0.09	−0.047±0.023	0.076±0.021
	1.00 –	1.50	1.23	20.4	1.09±0.11	−0.015±0.026	0.064±0.024
	1.50 –	2.00	1.72	11.7	1.20±0.15	−0.071±0.037	0.144±0.032
	2.00 –	6.00	2.60	11.1	0.97±0.15	0.026±0.041	0.198±0.033

Table 5: Parameters λ, μ, and ν in the CS frame as a function of $\sqrt{\tau}$

$\sqrt{s}$ [GeV]	Interval		$\langle\sqrt{\tau}\rangle$	Events ($\times 10^3$)	λ	μ	ν
16.2	0.24 –	0.28	0.26	19.1	1.08±0.13	−0.023±0.029	0.088±0.024
	0.28 –	0.34	0.31	15.4	1.08±0.13	0.024±0.032	0.112±0.027
	0.34 –	0.40	0.37	7.1	0.68±0.19	−0.013±0.044	0.039±0.038
	0.40 –	0.50	0.44	4.1	1.21±0.26	0.058±0.059	0.082±0.052
19.1	0.20 –	0.24	0.22	53.5	0.79±0.07	0.039±0.017	0.108±0.015
	0.24 –	0.29	0.26	50.3	0.79±0.07	0.043±0.017	0.081±0.015
	0.29 –	0.34	0.31	26.0	0.87±0.10	0.003±0.023	0.052±0.021
	0.34 –	0.43	0.37	17.6	1.02±0.11	−0.031±0.028	0.077±0.027
23.2	0.16 –	0.19	0.18	26.3	0.99±0.10	−0.032±0.025	0.157±0.021
	0.19 –	0.24	0.21	33.7	0.99±0.09	−0.002±0.022	0.099±0.019
	0.24 –	0.29	0.26	15.6	1.17±0.12	−0.050±0.031	0.062±0.027
	0.29 –	0.36	0.32	8.1	0.90±0.16	−0.053±0.039	−0.015±0.038

Table 6: Parameters λ, μ, and ν in the CS frame as a function of y

$\sqrt{s}$ [GeV]	Interval		⟨y⟩	Events ($\times 10^3$)	λ	μ	ν
16.2	−0.50 –	−0.05	−0.14	7.9	0.55±0.39	−0.029±0.065	0.034±0.037
	−0.05 –	0.10	0.03	11.0	0.90±0.16	−0.002±0.036	0.081±0.034
	0.10 –	0.20	0.15	8.6	0.79±0.15	0.011±0.036	0.105±0.038
	0.20 –	0.30	0.25	7.8	0.88±0.16	0.001±0.039	0.089±0.038
	0.30 –	0.70	0.40	10.5	1.93±0.24	0.052±0.052	0.118±0.030
19.1	−0.25 –	0.20	0.09	36.0	0.92±0.13	−0.002±0.027	0.059±0.018
	0.20 –	0.35	0.28	36.3	0.77±0.08	0.032±0.019	0.070±0.019
	0.35 –	0.45	0.40	25.4	0.92±0.09	0.026±0.022	0.143±0.022
	0.45 –	0.55	0.50	21.9	0.68±0.09	0.005±0.023	0.081±0.024
	0.55 –	0.95	0.65	28.0	0.86±0.13	0.031±0.031	0.089±0.019
23.2	−0.20 –	0.25	0.14	18.3	0.70±0.20	0.004±0.039	0.080±0.025
	0.25 –	0.40	0.33	19.1	0.84±0.11	−0.010±0.027	0.131±0.025
	0.40 –	0.50	0.45	14.3	1.00±0.12	−0.049±0.030	0.139±0.030
	0.50 –	0.60	0.55	13.0	1.02±0.12	−0.053±0.030	0.067±0.030
	0.60 –	1.00	0.71	18.9	0.91±0.14	−0.018±0.032	0.073±0.024

Table 7: Parameters λ, μ, and ν in the CS frame as a function of x_1

$\sqrt{s}$ [GeV]	Interval		⟨x_1⟩	Events ($\times 10^3$)	λ	μ	ν
16.2	0.00 –	0.35	0.29	24.3	1.01±0.11	−0.051±0.027	0.068±0.022
	0.35 –	0.50	0.41	17.9	1.18±0.12	0.031±0.029	0.107±0.025
	0.50 –	0.60	0.54	2.9	0.83±0.31	0.024±0.076	0.181±0.060
19.1	0.00 –	0.35	0.29	54.0	0.82±0.08	0.034±0.018	0.080±0.015
	0.35 –	0.50	0.42	66.0	0.83±0.06	0.022±0.015	0.085±0.013
	0.50 –	0.60	0.54	19.9	0.93±0.12	0.056±0.030	0.096±0.024
	0.60 –	0.70	0.64	7.8	0.87±0.21	−0.113±0.048	0.080±0.037
	0.70 –	1.10	0.77	3.5	0.90±0.35	−0.036±0.079	0.153±0.056
23.2	0.00 –	0.35	0.28	35.1	1.08±0.10	−0.055±0.023	0.125±0.019
	0.35 –	0.50	0.42	33.1	0.97±0.08	−0.015±0.020	0.108±0.019
	0.50 –	0.60	0.54	10.9	0.93±0.16	−0.064±0.037	0.030±0.032
	0.60 –	0.70	0.64	4.9	0.93±0.25	−0.141±0.058	0.009±0.047
	0.70 –	1.10	0.80	3.9	0.54±0.30	−0.079±0.067	0.074±0.052

Figure Captions

Fig. 1 Parameters λ, μ, and ν as a function of $\sqrt{s}$ in the CS frame. The error bars correspond to the statistical uncertainties only. The horizontal bars correspond to the momentum bite ($\pm 10\%$). The dashed horizontal lines are the averages over the three points.

Fig. 2 **a, b, c** Parameters λ, μ, and ν as a function of ρ in the CS frame. **a** 140 GeV/c; **b** 194 GeV/c; **c** 286 GeV/c. The error bars correspond to the statistical uncertainties only. The horizontal bars give the size of each interval. For ν, the dot-dashed curve is the fit to the empirical relation (4); for λ, it is given by (5).

Fig. 3 **a, b, c** Parameters λ, μ, and ν as a function of P_T in the CS frame. **a** 140 GeV/c; **b** 194 GeV/c; **c** 286 GeV/c. The error bars correspond to the statistical uncertainties only. The horizontal bars give the size of each interval. The dashed curves are the predictions of perturbative QCD [3].

Fig. 4 **a, b, c** Parameters λ, μ, and ν as a function of $\sqrt{\tau}$ in the CS frame. **a** 140 GeV/c; **b** 194 GeV/c; **c** 286 GeV/c. The error bars correspond to the statistical uncertainties only. The horizontal bars give the size of each interval.

Fig. 5 **a, b, c** Parameters λ, μ, and ν as a function of y in the CS frame. **a** 140 GeV/c; **b** 194 GeV/c; **c** 286 GeV/c. The error bars correspond to the statistical uncertainties only. The horizontal bars give the size of each interval.

Fig. 6 **a, b, c** Parameters λ, μ, and ν as a function of x_1 in the GJ frame. **a** 140 GeV/c; **b** 194 GeV/c; **c** 286 GeV/c. The error bars correspond to the statistical uncertainties only. The horizontal bars give the size of each interval.

Fig. 7 Parameter λ as a function of x_1 in the GJ frame. The data are averaged over the three beam momenta. The error bars correspond to the statistical uncertainties only. The horizontal bars give the size of each interval. The dashed curve is a fit to the higher-twist hypothesis [2], and the dot-dashed one a straight-line fit.

Fig. 8 **a, b, c** Parameters λ, μ, and ν as a function of **a** M, **b** P_T, and **c** x_1 in the CS frame. Open circles: 286 GeV/c deuterium data. Full circles: 286 GeV/c tungsten data. The error bars correspond to the statistical uncertainties only.

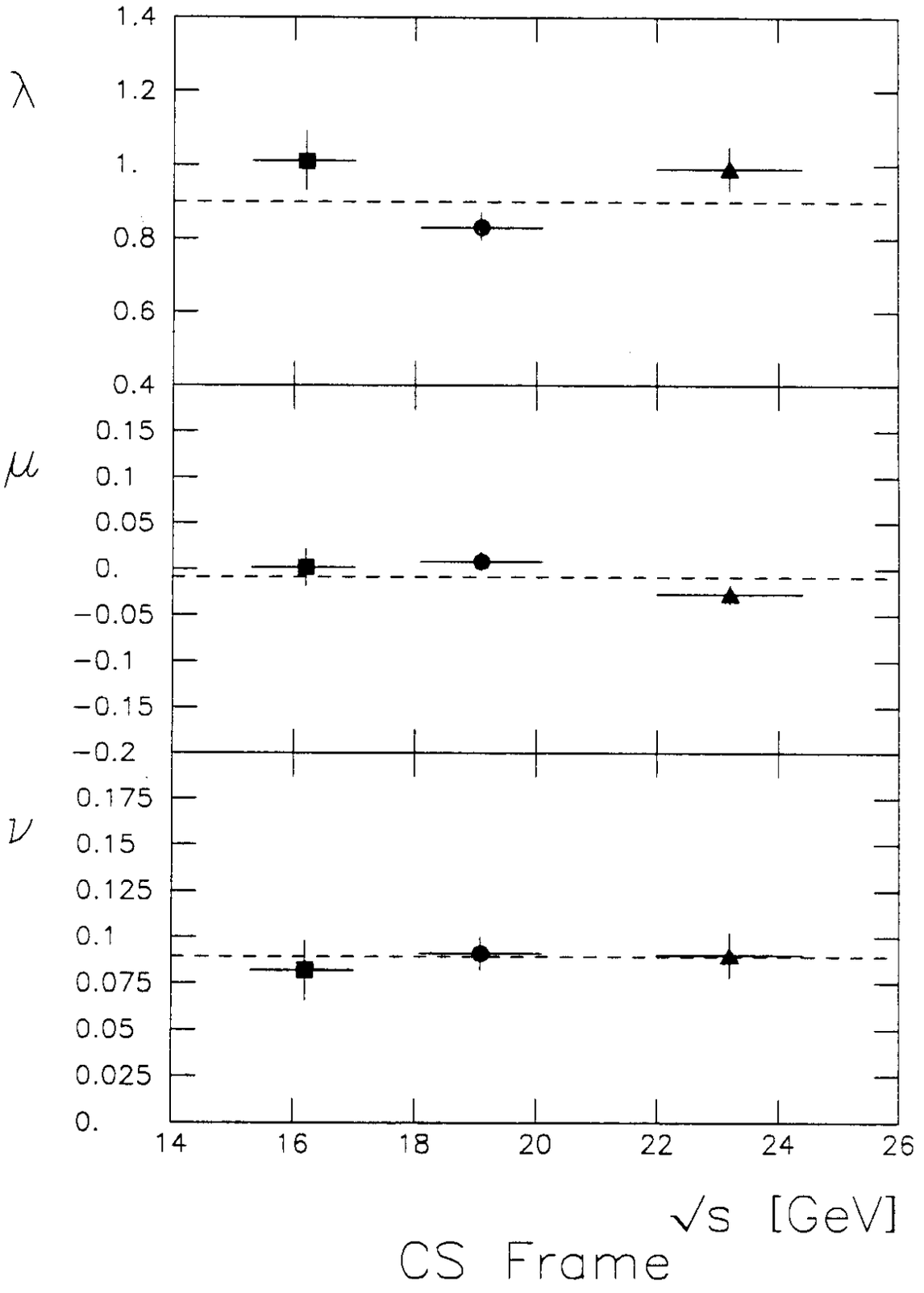
λ
1.4
1.2
1.
0.8
0.6
0.4
μ
0.15
0.1
0.05
0.
−0.05
−0.1
−0.15
−0.2
ν
0.175
0.15
0.125
0.1
0.075
0.05
0.025
0.
14
16
18
20
22
24
26
√s [GeV]
CS Frame

Fig. 1

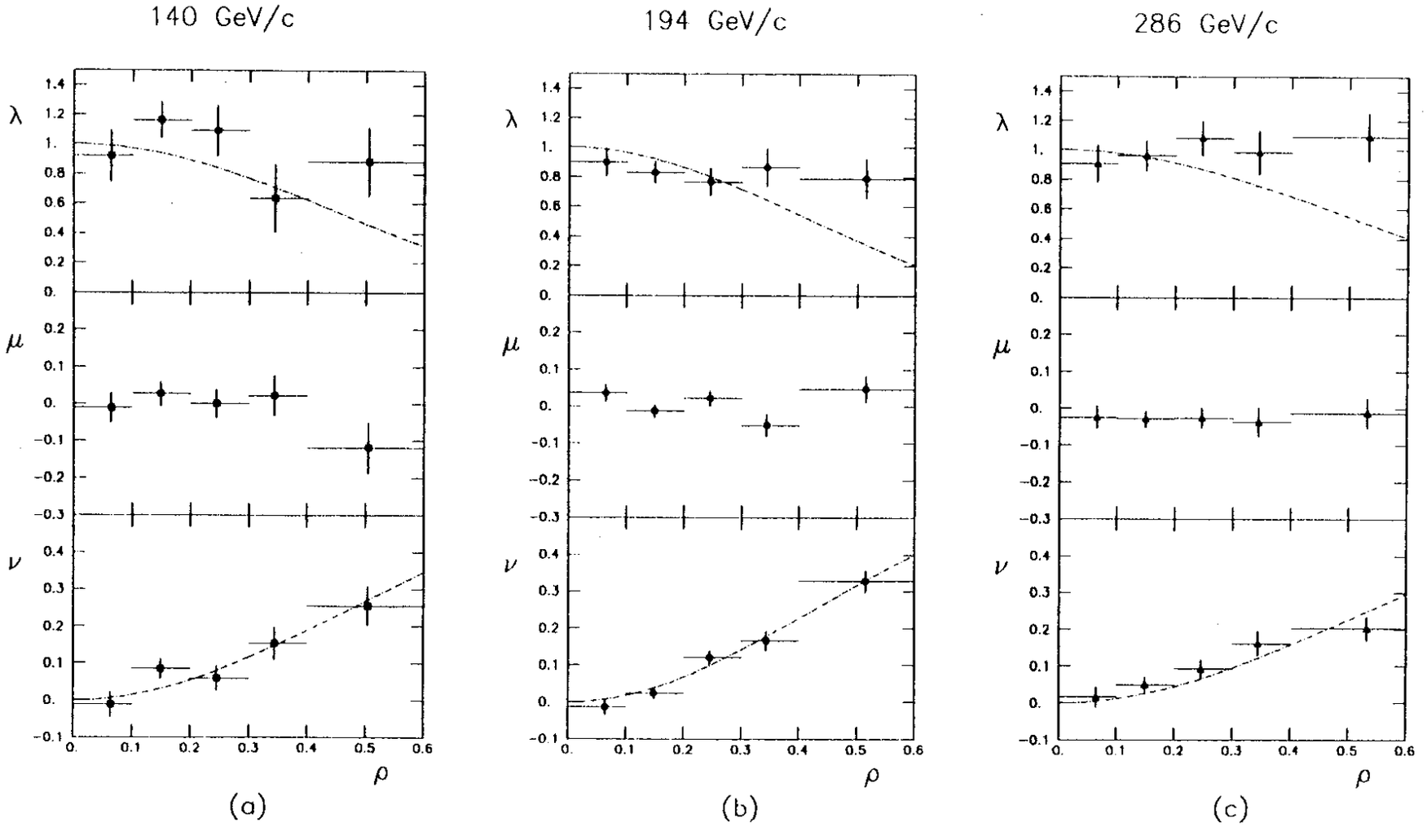

Fig. 2

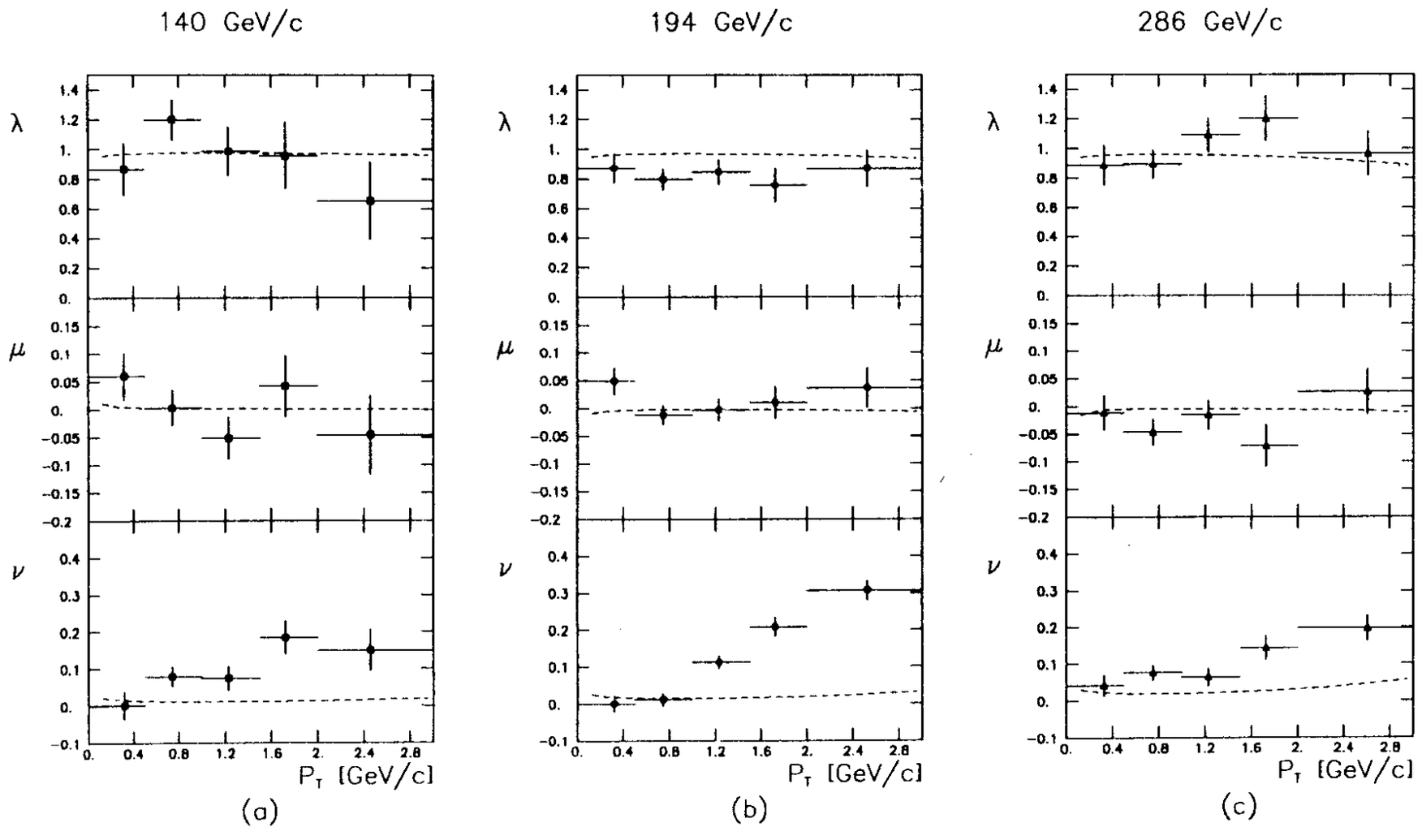

Fig. 3

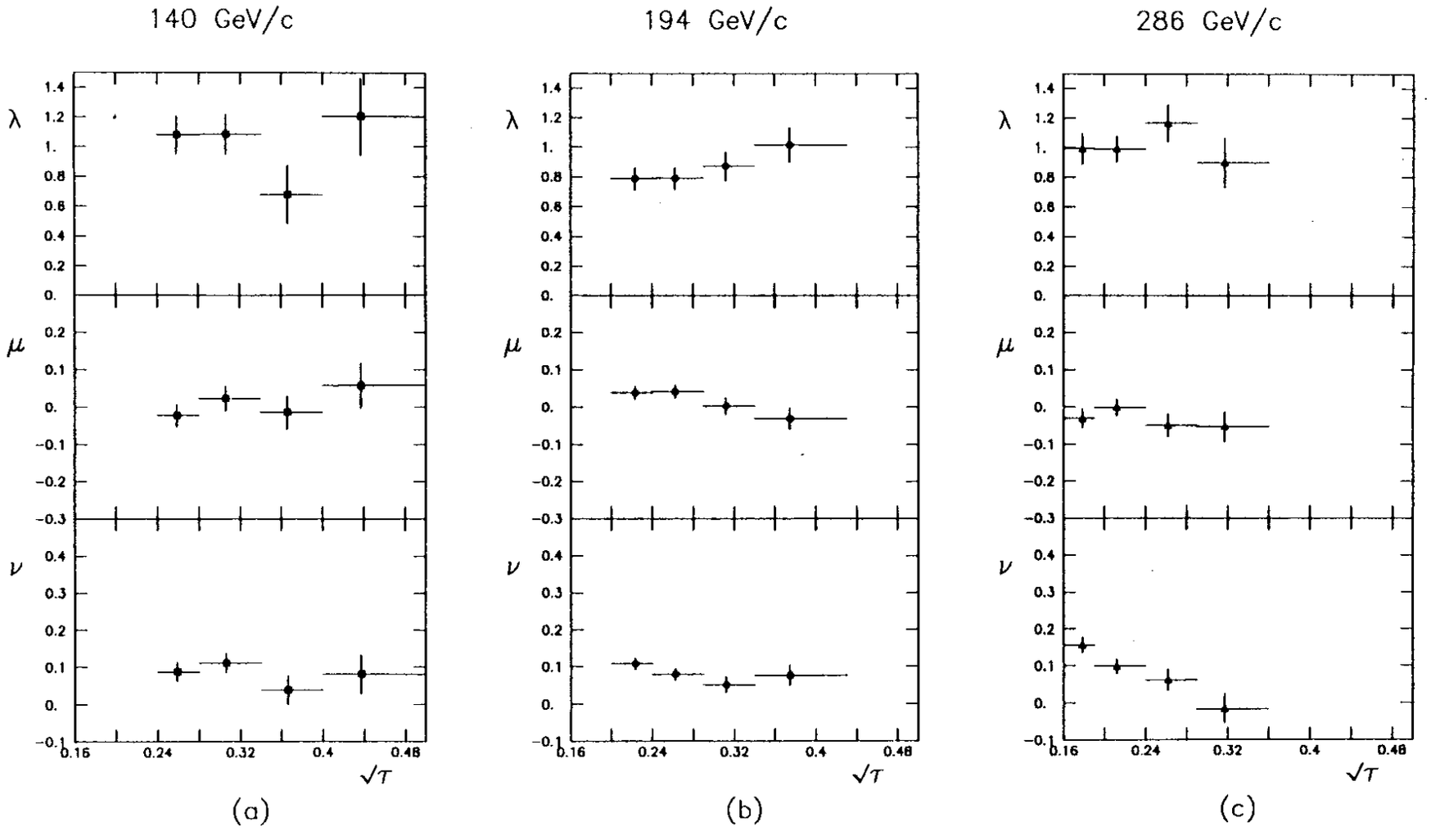

Fig. 4

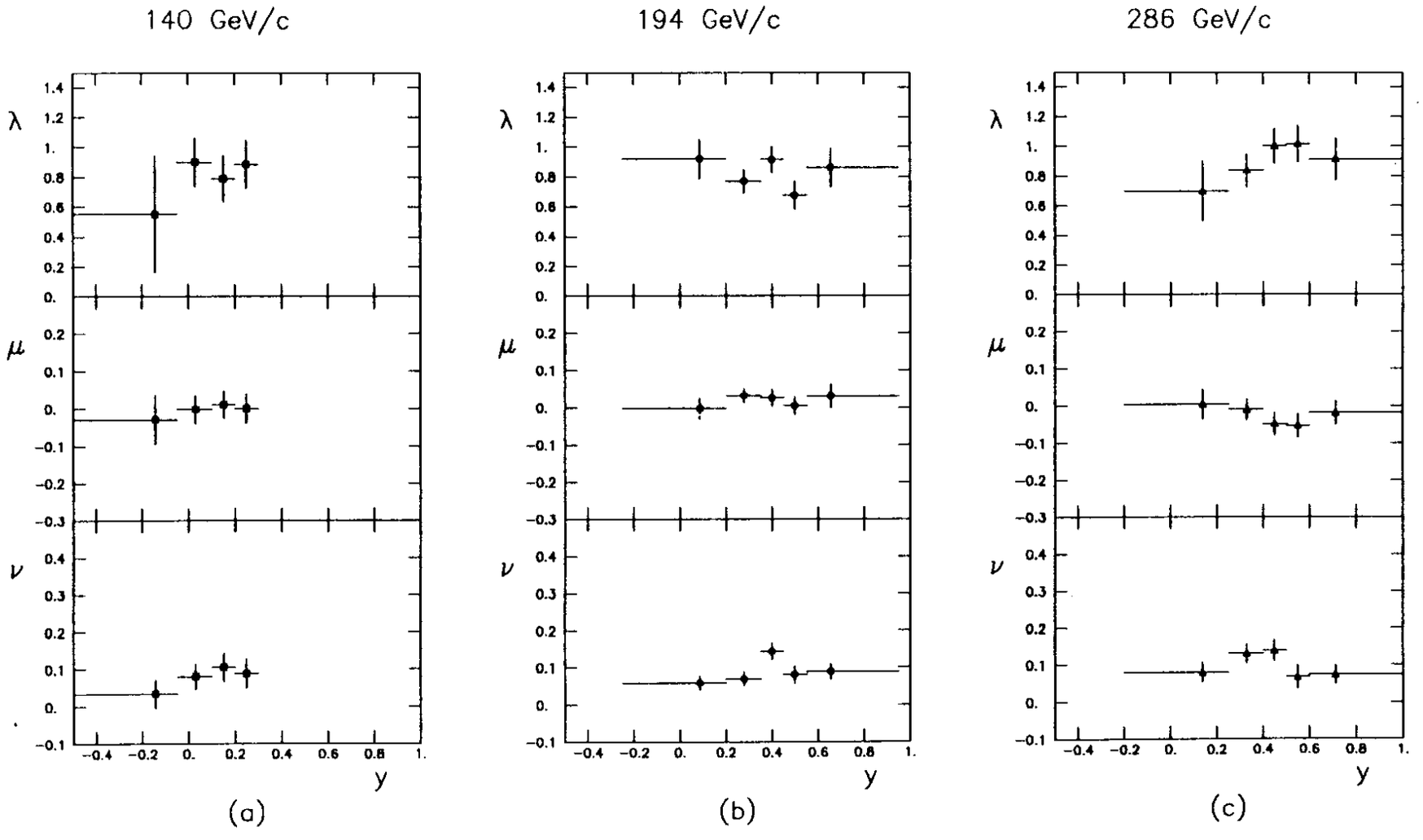

Fig. 5

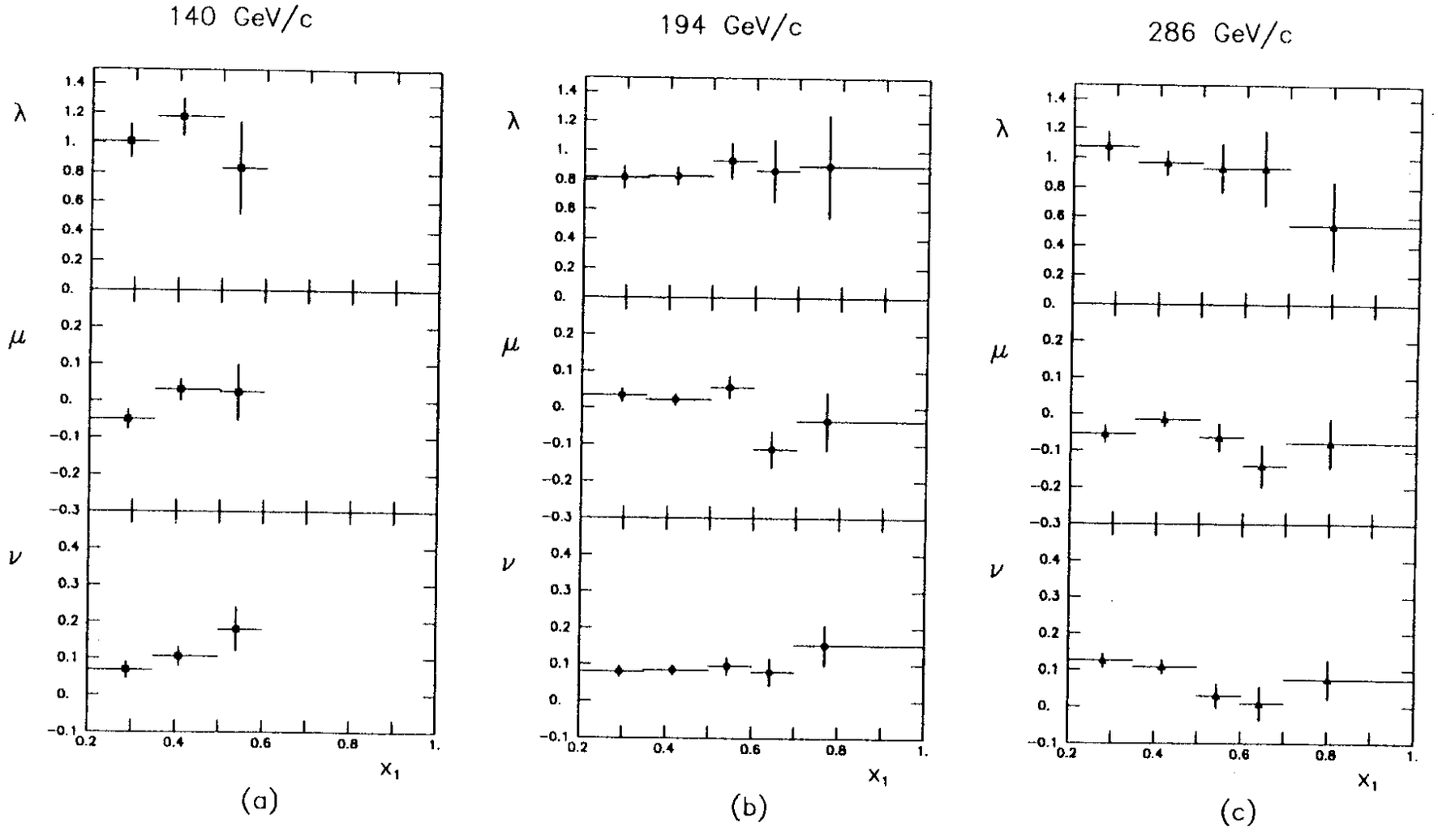

Fig. 6

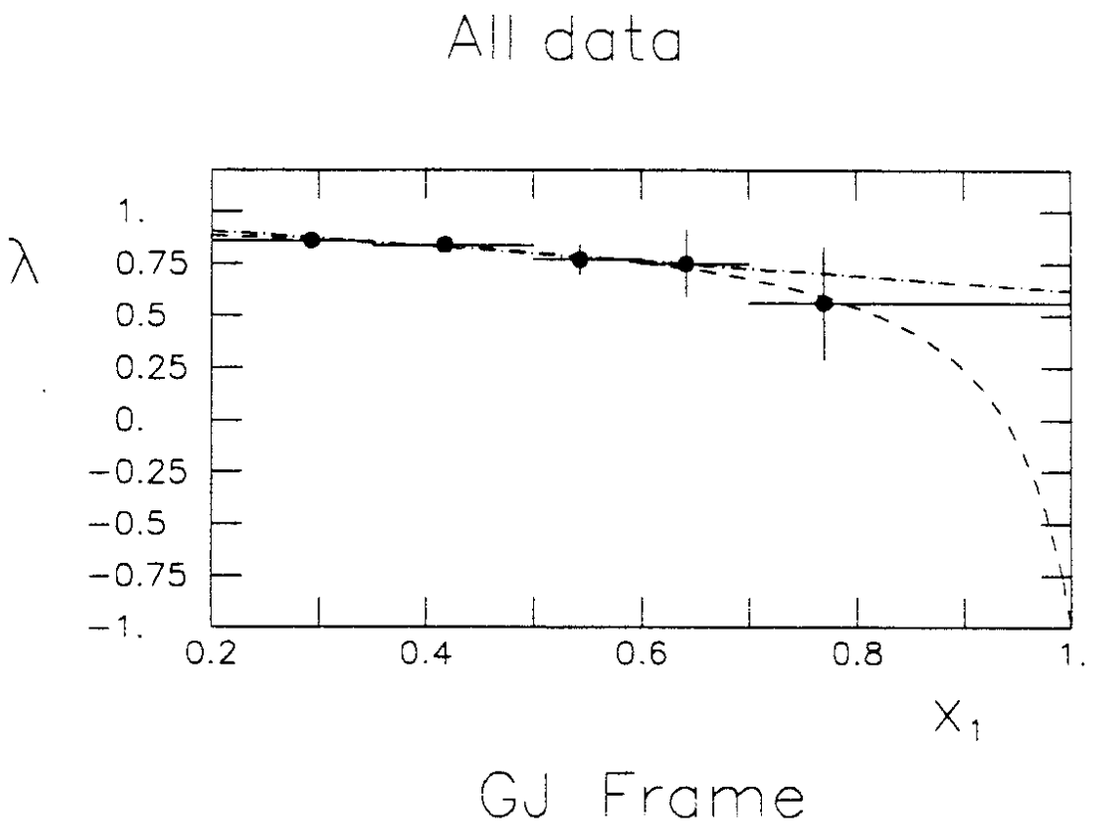

Fig. 7

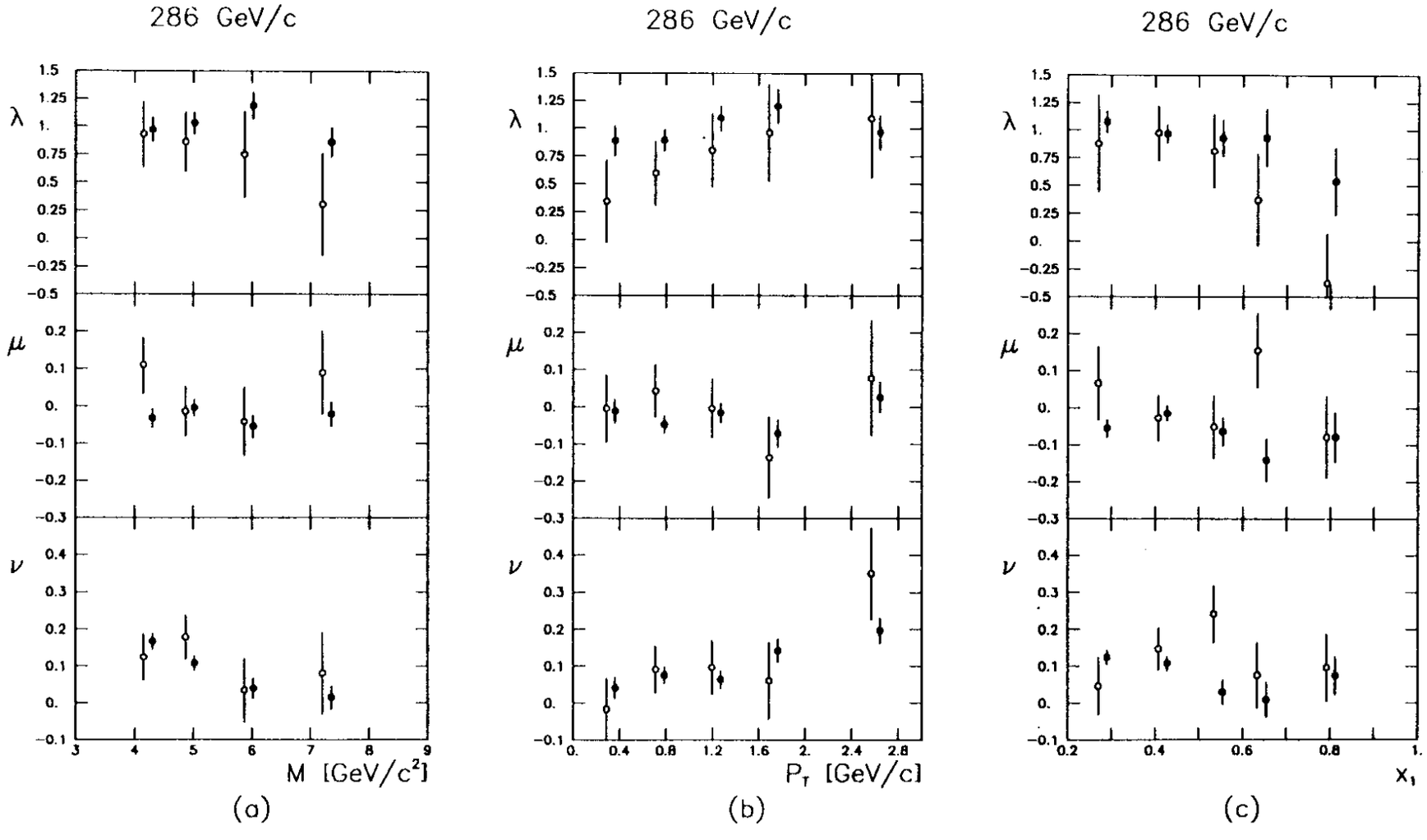

Fig. 8